A Check of the Total Number of τ-pair Events Decayed from $\psi^{'}$ in the Measurement of the $Br(\psi^{'} \to \tau^{+}\tau^{-})$

Yu Chunxu, Luo Yong, Qi Nading, Cui Xiangzhong, Gu Yifan

Institute of the High Energy Physics

Academia Sinica

Beijing 100039, P. R. China

June 7, 1996

1 Introduction

1.1 The physics significance

Up to now, experimental evidence suggests that the τ particle is a conventional lepton, which behaves itself like other two charged leptons — electron and μ, obeying the rule of the $e-\mu-\tau$ universality hypothesis. In the $c\bar{c}$ system, the $\psi^{'}$ provides an unique opportunity to compare the three generation leptons by studying its leptonic decay. According to the theory, the relations between the branching ratios of the decay modes $\psi^{'} \to e-, \mu-$ and $\tau - pair$, $Br_{ee}, Br_{\mu\mu}$ and $Br(\psi^{'} \to \tau\tau)$ are given by

$$\frac{Br(\psi^{'} \to \tau\tau)}{0.3885} \approx Br_{\mu\mu} \approx Br_{ee} \tag{1}$$

Previous experiments have yielded the measurements of Br_{ee} and $Br_{\mu\mu}$, but no $Br(\psi^{'} \to \tau\tau)$. By use of the 93/94 $\psi^{'}$ data, we have measured the value of the $Br(\psi^{'} \to \tau\tau)$, which was reported in the BES Annual Meeting, the HEP-Glasgow in 1994 and so on. But before formal publication, the measurement of the $Br_{\tau\tau}$ must be checked.

1.2 Our main task

This memo will clarify and solve some important problems as follows:

In the previous measurement of the total $\tau - pair$ event number $N_{\tau\tau}$, we used

a. the 93/94 $\psi^{'}$ filtered data collected by BES, which place a restriction on the tracks in the SC. We worry about that might result in the loss of the $N_{\tau\tau}$;

b. the 92 Ds data collected by BES, used as determining the detection efficiency ε_d, which are divided into two datasets, each with different threshold values set for the MDC trigger(see Table 1). We are afraid that lead to the loss of the ε_d, namely the increasement of the $N_{\tau\tau}$.

Our way to deal with the above problems is

a. using the 93/94 $\psi^{'}$ unfiltered data reconstructed by USA instead of the filtered data;

b. using the 93 Ds low threshold data, instead of the previously used 92 Ds data(see Table 1).

Table 1 the different thresholds between these datasets

datasets	range	threshold (MDC)
92 Ds data	3097 — 3450	875
	3739 — 3966	625
93 Ds data	4489 — 4640	625
	4750 — 5698	
93/94 $\psi^{'}$ data	5738 — 6059	625

Certainly, in the course of checking, we also make some improvements on other conditions. For example, the isolated photon should be the same as that in the measurement of the τ-mass, that is, it has $Esc \geq 60MeV$, and is separated from the nearest charged track by $\theta_{open} > 12°$.

2 Formulae used in the measurement

2.1 The formula for measuring $Br(\psi^{'} \to \tau\tau)$

$$Br(\psi^{'} \to \tau\tau) = \frac{N_{\tau\tau} - \sigma_{Q+I} \bullet L}{N_{\psi'}} \tag{2}$$

where $N_{\tau\tau}$ is the total τ-pair event number; σ_{Q+I} is the sum of the cross section of the QED generating τ-pair and that of the interference part; L is the integrated luminosity at the $\psi^{'}$ resonance; $N_{\psi'}$ is the number of the produced $\psi^{'}$ events.

2.2 The formula for measuring $N_{\tau\tau}$

The $\tau\tau$ events are identified by means of the six topologies, $e\mu, eh, ee, \mu h, e\rho$ and $\mu\rho$. By using the observed event number n for each of the six topologies, $N_{\tau\tau}$ is expressed as

$$N_{\tau\tau} = \frac{n}{B \bullet \varepsilon_d \bullet \varepsilon_t} \tag{3}$$

where B is the branching ratio of the relevant $\tau\tau$ decay topology; ε_d and ε_t are respectively the detection and trigger efficiency of the relevant channel.

In fact, to evaluate ε_d we first measure the $\varepsilon_d^{'}$ at $\sqrt{s} = 4.03GeV$, which is expressed as

$$\varepsilon_d^{'} = \frac{n^{'}}{B \bullet \sigma_{QED}^{'} \bullet L^{'}} \tag{4}$$

where $n^{'}$ is the observed event number; $\sigma_{QED}^{'}$ is the cross section of the QED generating τ-pair at $\sqrt{s} = 4.03GeV$; $L^{'}$ is the accumulated luminosity at $\sqrt{s} = 4.03GeV$. Monte Carlo simulations of the BES detector have been made to determine the ratio $\lambda = \varepsilon_d/\varepsilon_d^{'}$, thus the above formula(3) will be simplified as follows:

$$N_{\tau\tau} = \frac{n \bullet \sigma_{QED}^{'} \bullet L^{'}}{n^{'} \bullet \lambda \bullet \varepsilon_t} \tag{5}$$

3 Analysis method

3.1 The preselection of $\tau^+\tau^-$ events

The six topologies are

$$\tau\tau \rightarrow e\mu, eh, ee, \mu h, e\rho \text{ and } \mu\rho$$

where h only stands for π and K particles.

Each of these channels has two opposite charged tracks; for the decay modes $e\mu, eh, ee$ and μh, there should be no isolated photons, and for the $e\rho$ and $\mu\rho$ modes, there should be only two γs coming from π^0 which is decayed from $\rho^{\pm}$.

The preselection conditions are

- $|x| \leq 1.5cm, |y| \leq 1.5cm, |z| \leq 20cm$;
- $N_{chrg} = 2, \sum q_i = 0, M_{fit} = 2$; $N_{neu} \leq 20$;
- $2.5^\circ \leq acol \leq 177.5^\circ$; $acop \geq 6^\circ$;
- if a neutral track in one event has $E_{sc} > 0.1GeV$, and is separated from the nearest charged track by $\theta_{open} > 20^\circ$, the event is demanded $acol > 5^\circ, acop > 10^\circ; N_{neu} \geq 2, E_{sc} \geq 0.03GeV$ and $0.035GeV/C^2 \leq M_{\gamma\gamma} \leq 0.3GeV/C^2$.

3.2 The selection criteria of $\tau^+\tau^-$ events

We first introduce the criteria to identify the particles involved, that is, e, μ and π ,h particles.

a. e

- $0.8 \leq \beta \leq 1.5$;
- $|\cos\theta| \leq 0.75$;
- no μ-hits;
- when $P \leq 350MeV, \beta \geq 1$ and $Esc/P \geq 0.7$;
- when $350MeV < P \leq 700MeV, \beta > 0.9$ and $idsh \geq -1$ and ($xspi \geq 2.5|xse|$ or $0 \leq xse \leq 10$);
- when $P > 700MeV$, ($Esc \geq 500MeV$ and $\beta \geq 0.9$ and $idsh \geq 1$) or ($Esc \geq 600MeV$ and $idsh \geq -3$).

b. μ

one layer μ-hit: $|Av| \leq 4$ and $|Az| \leq 6$.

first level μ-cut: having at least one layer μ-hit with two tube μ-hits;

second level μ-cut: having at least two layer μ-hits or the second layer and third layer having a μ-hit with two tube μ-hits.

- if a charged particle satisfies the second level μ-cut, it is identified as a μ;
- when $P_\pi lo \leq P \leq P_\pi hi$ or $\mu_{require} \leq 1$, if the charged particle satisfies the first level μ-cut and it has $Esc \leq 450MeV$, it is also identified as a μ.

c. π

- $|\cos\theta| \leq 0.75$;
- no μ-hits;
- when $P \leq 350MeV$, $0.6 \leq \beta \leq 0.85$ and $Esc/P \leq 0.5$;
- when $350MeV < P \leq 700MeV$, $0.8 \leq \beta \leq 1.5$ and $idsh \leq -2$ and ($xspi \leq 0$ if $xse \leq 0$ or $|xse| \geq 2.5|xspi|$);
- when $P > 700MeV$, $0.85 \leq \beta \leq 1.5$ and $Esc \leq 400MeV$ and $idsh \leq -1$.

d. h

Because the momentum of π directly decayed from τ may be up to 1.2 GeV, it may be difficult to separate π with large momentum from K. So we indentify h particle (h stand for π and K), not separating them.

- $|\cos\theta| \leq 0.75$;
- no μ-hits;
- $|xse| \leq 0$ or $|xspi| \leq 0.5$ or $|xsk| \leq 0.5$;
- $|xspi| \leq 2.5|xse|$ or $|xsk| \leq 2.5|xse|$;
- $0.75 \leq \beta \leq 1.5$;
- $Esc \leq 400MeV$;
- $idsh \leq -1$.

The selection criteria are divided into two parts.
The common conditions for selecting the six channels are:

- $|x| \leq 1.5cm, |y| \leq 1.5cm, |z| \leq 15cm$;
- the isolated photon is: $Esc \geq 60MeV$, the angle between it and the charged track nearest to it $\theta_{open} \geq 12°$;
- no isolated TOF. The isolated TOF means that there are some hits in the TOF, but they don't match any tracks in MDC. $T_{qual} = 1, 2$ or 7.

The different conditions for selecting the six channels are determined by studying the Monte Carlo data of $\psi' \to \tau\tau$, 93/94 ψ' data and J/ψ real data (the J/ψ data are used to estimate the $q\bar{q}$ background). The M.C. simulation data are compared to the 93/94 ψ' data as shown in the Figures from 1st to 15th.

$e\mu$ channel

- one track is an e, the other a μ, those momenta required $P_{min} \leq P_{e,\mu} \leq P_{max}$;
- no isolated photon;
- $acop \geq 10°$;
- $10° \leq acol \leq 170°$;
- $ptem \geq 0.1$.

eh channel

- one track is an e, the other a h, those momenta required $P_{min} \leq P_e \leq P_{max}, P_h lo \leq P_h \leq P_h hi$, $P_h lo = min(P_K lo, P_\pi lo)$, $P_h hi = max(P_K hi, P_\pi hi)$;
- no isolated photon;

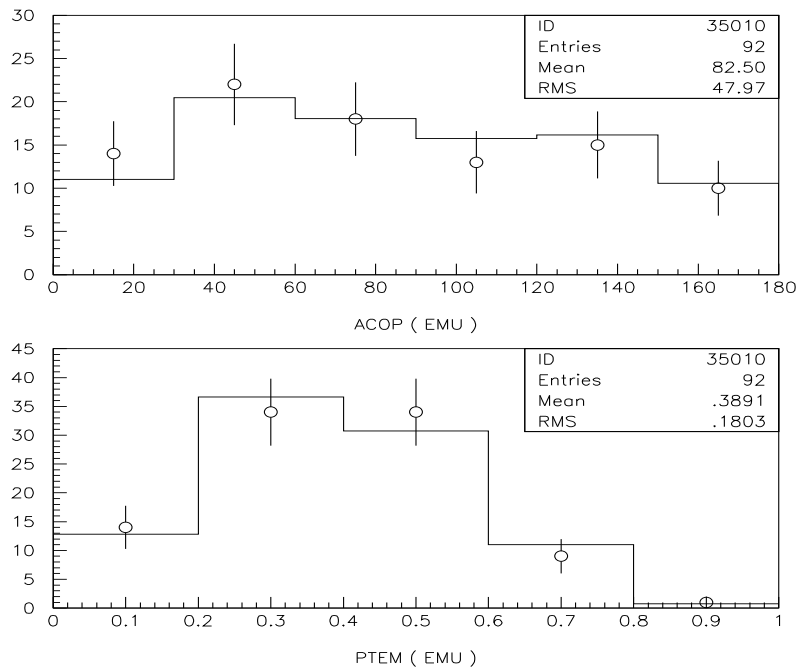

Figure 1: The distributions in ACOP and PTEM for the $\tau^+\tau^- \to e\mu$ candidate events (points) compared to that for the $\tau\tau$ Monte Carlo events subjected to the same selection criteria (histogram) and normalized to the data.

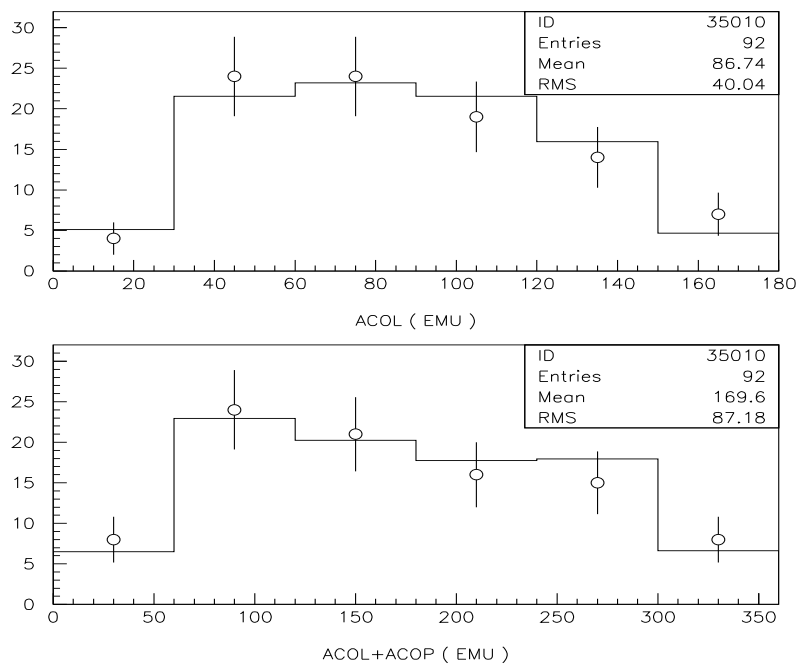

Figure 2: The distributions in ACOL and ACOL+ACOP for the $\tau^+\tau^- \to e\mu$ candidate events (points) compared to that for the $\tau\tau$ Monte Carlo events subjected to the same selection criteria (histogram) and normalized to the data.

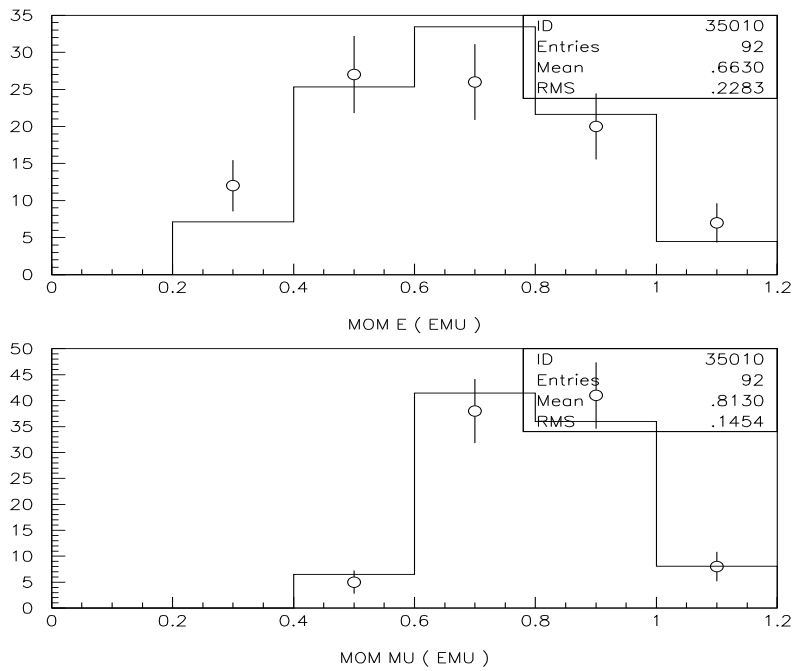

Figure 3: The distributions in the momenta of e and μ for the $\tau^+\tau^- \to e\mu$ candidate events (points) compared to that for the $\tau\tau$ Monte Carlo events subjected to the same selection criteria (histogram) and normalized to the data.

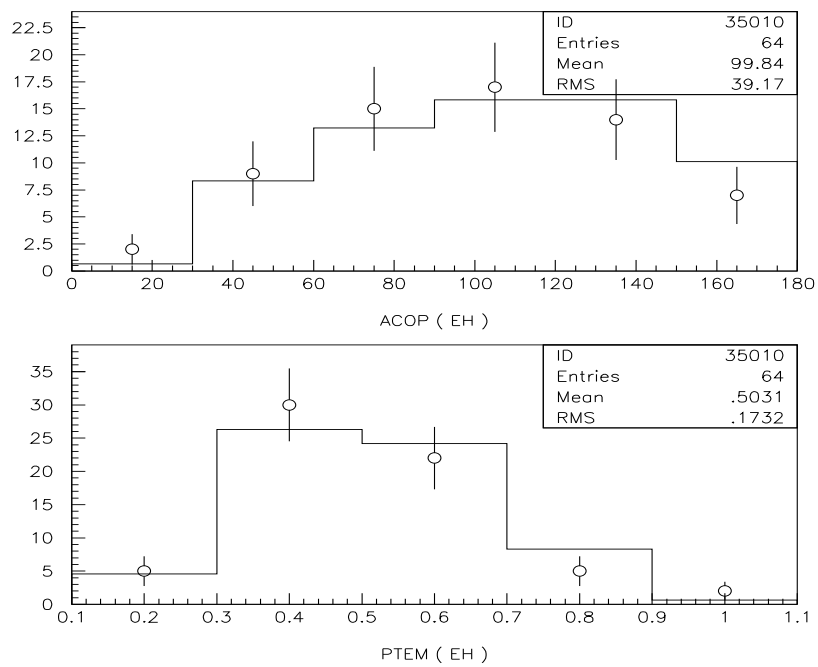

Figure 4: The distributions in the ACOP and PTEM for the $\tau^+\tau^- \to eh$ candidate events (points) compared to that for the $\tau\tau$ Monte Carlo events subjected to the same selection criteria (histogram) and normalized to the data.

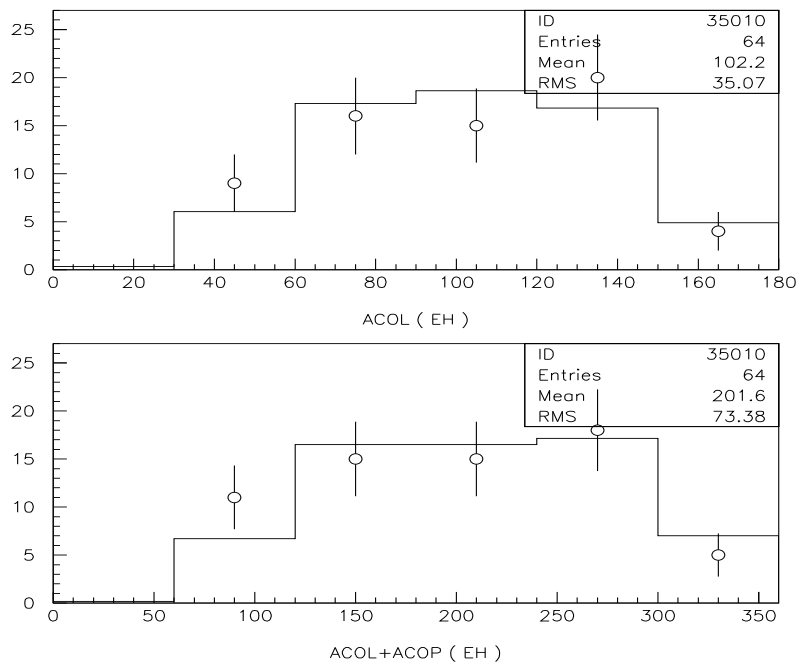

Figure 5: The distributions in the ACOL and ACOL+ACOP for the $\tau^+\tau- \rightarrow eh$ candidate events (points) compared to that for the $\tau\tau$ Monte Carlo events subjected to the same selection criteria (histogram) and normalized to the data.

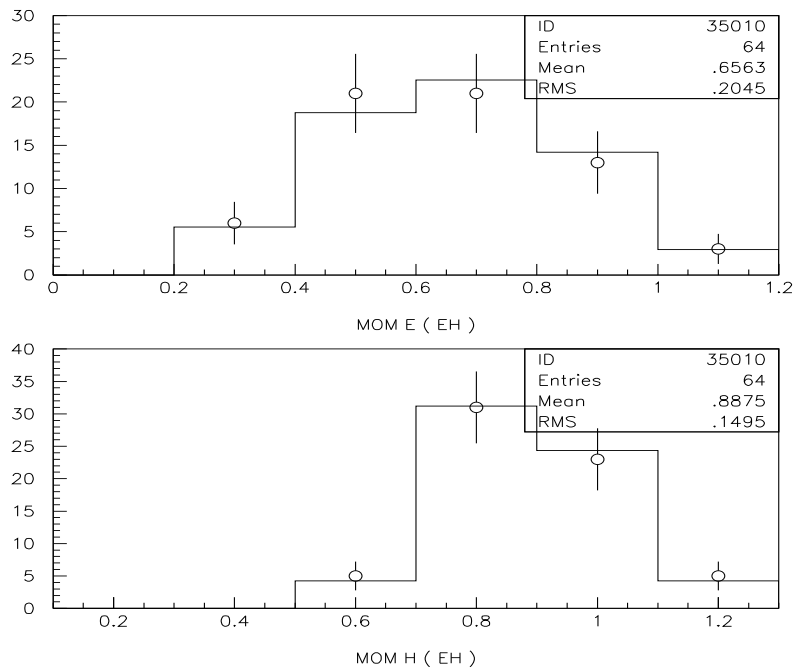

Figure 6: The distributions in the momenta of e and h for the $\tau^+\tau^- \rightarrow eh$ candidate events (points) compared to that for the $\tau\tau$ Monte Carlo events subjected to the same selection criteria (histogram) and normalized to the data.

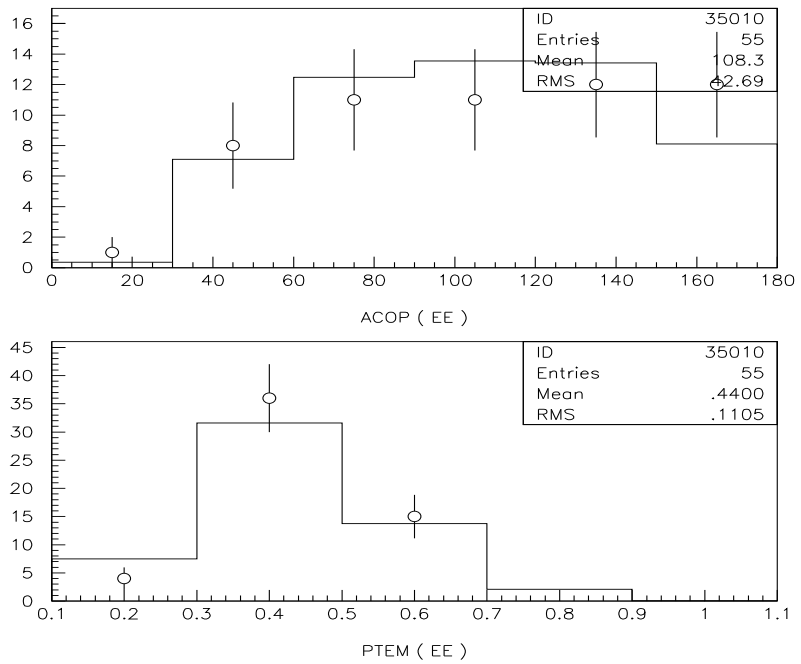

Figure 7: The distributions in the ACOP and PTEM for the $\tau^+\tau^- \rightarrow ee$ candidate events (points) compared to that for the $\tau\tau$ Monte Carlo events subjected to the same selection criteria (histogram) and normalized to the data.

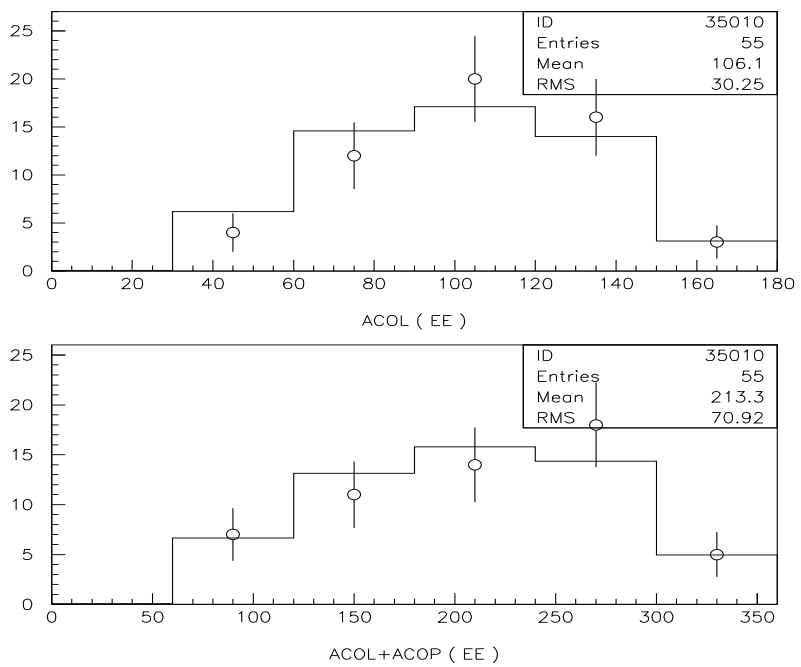

Figure 8: The distributions in the ACOL and ACOL+ACOP for the $\tau^+\tau^- \rightarrow ee$ candidate events (points) compared to that for the $\tau\tau$ Monte Carlo events subjected to the same selection criteria (histogram) and normalized to the data.

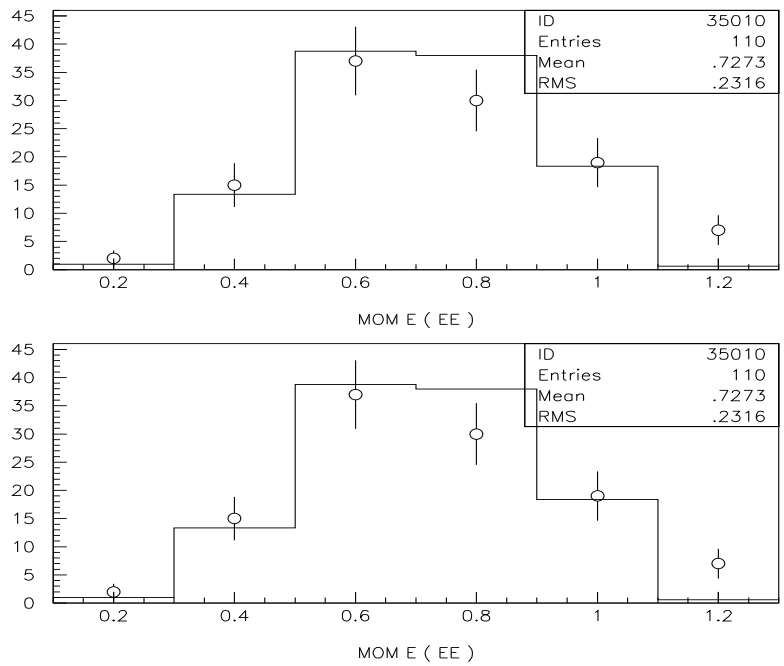

Figure 9: The distributions in the momenta of e for the $\tau^+\tau- \rightarrow ee$ candidate events (points) compared to that for the $\tau\tau$ Monte Carlo events subjected to the same selection criteria (histogram) and normalized to the data.

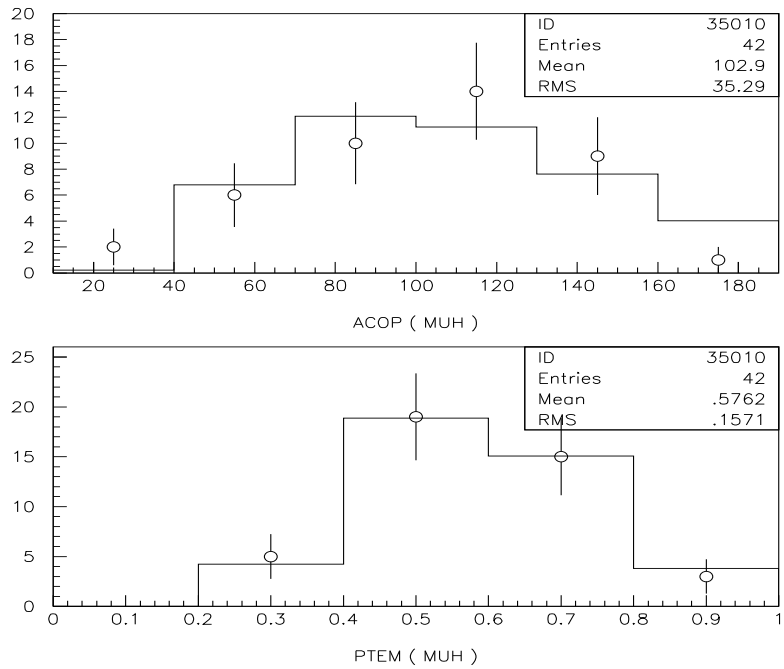

Figure 10: The distributions in the ACOP and PTEM for the $\tau^+\tau^- \rightarrow \mu h$ candidate events (points) compared to that for the $\tau\tau$ Monte Carlo events subjected to the same selection criteria (histogram) and normalized to the data.

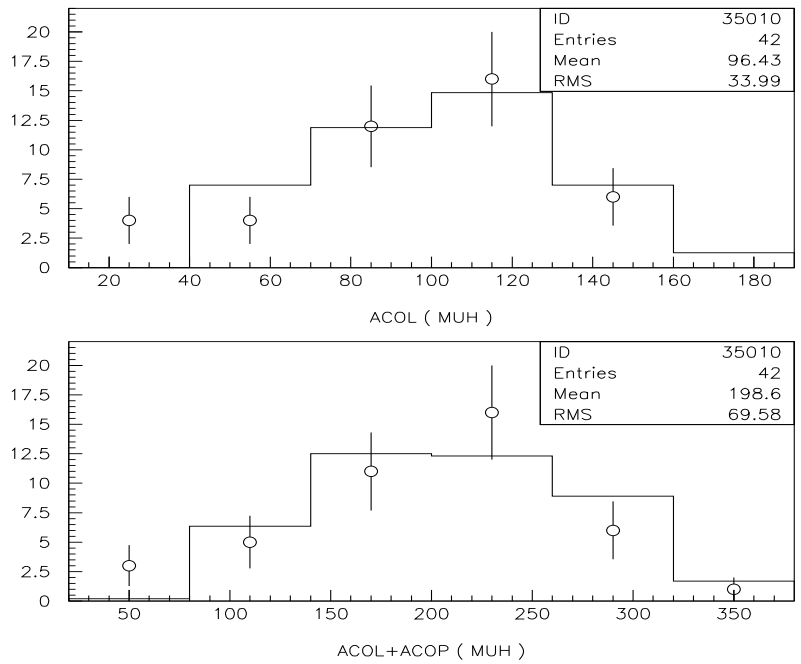

Figure 11: The distributions in the ACOL and ACOL+ACOP for the $\tau^+\tau^- \rightarrow \mu h$ candidate events (points) compared to that for the $\tau\tau$ Monte Carlo events subjected to the same selection criteria (histogram) and normalized to the data.

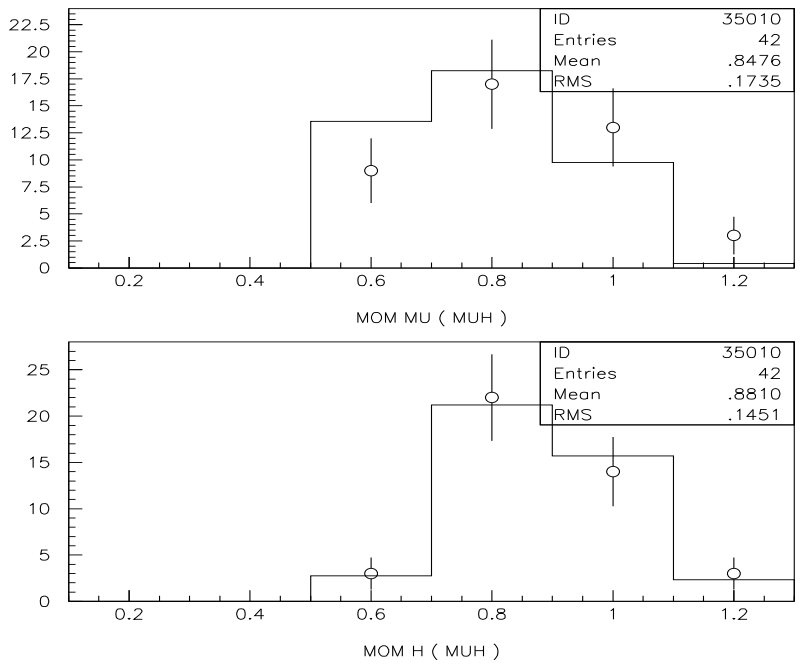

Figure 12: The distributions in the momtentua of μ and h for the $\tau 6+\tau^- \rightarrow \mu h$ candidate events (points) compared to that for the $\tau\tau$ Monte Carlo events subjected to the same selection criteria (histogram) and normalized to the data.

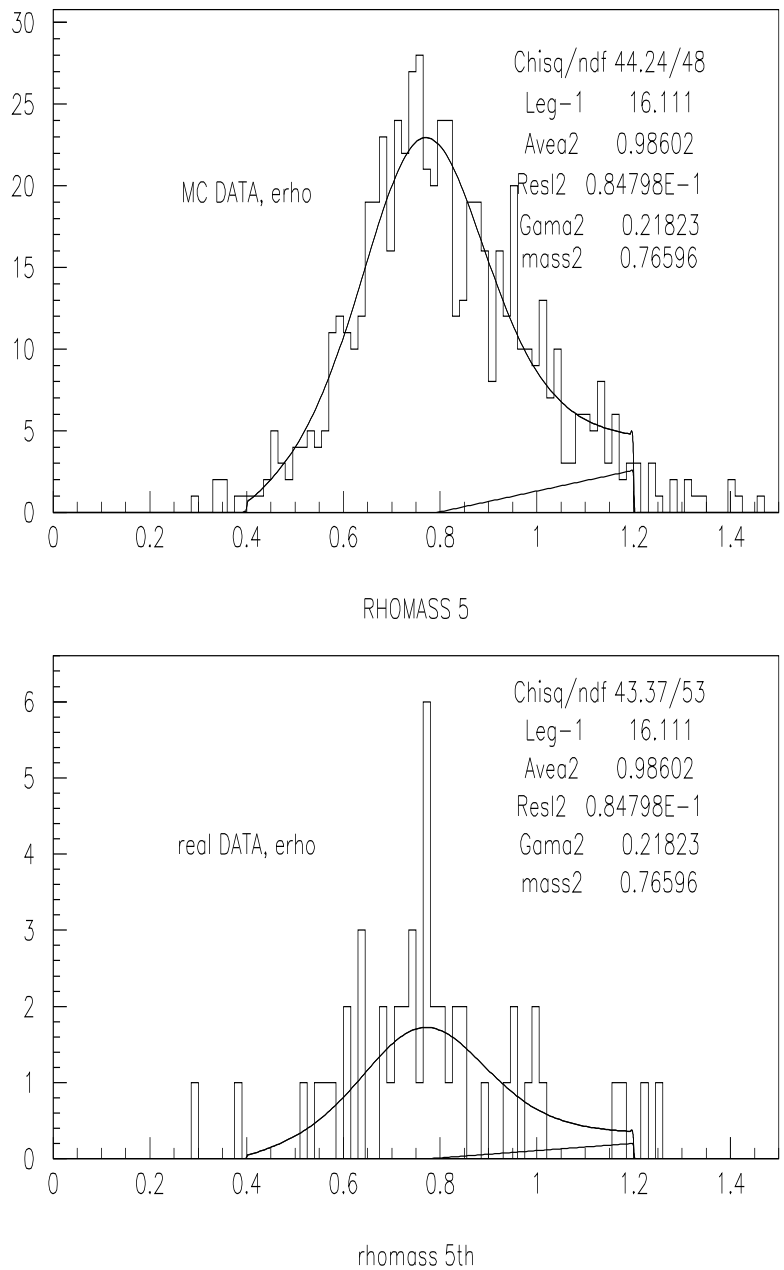

Figure 13: $e\rho$ channel. The curve above is obtained by fitting the M. C. simulation 10k $\tau\tau \rightarrow e\rho$ events; the curve below comes from above figure, being real data

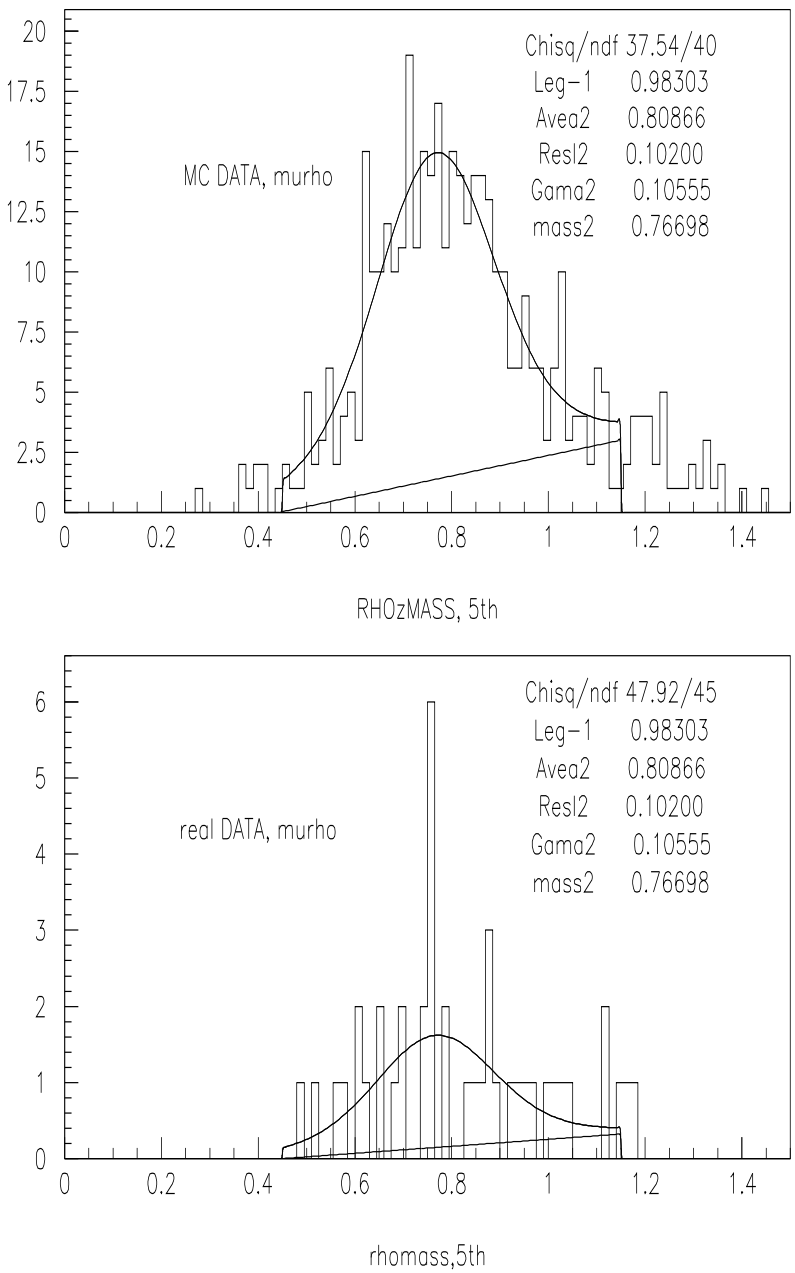

Figure 14: $\mu\rho$ channel. The curve above is obtained by fitting the M. C. simulation 10k $\tau\tau \to \mu\rho$ events; the curve below comes from above figure, being real data

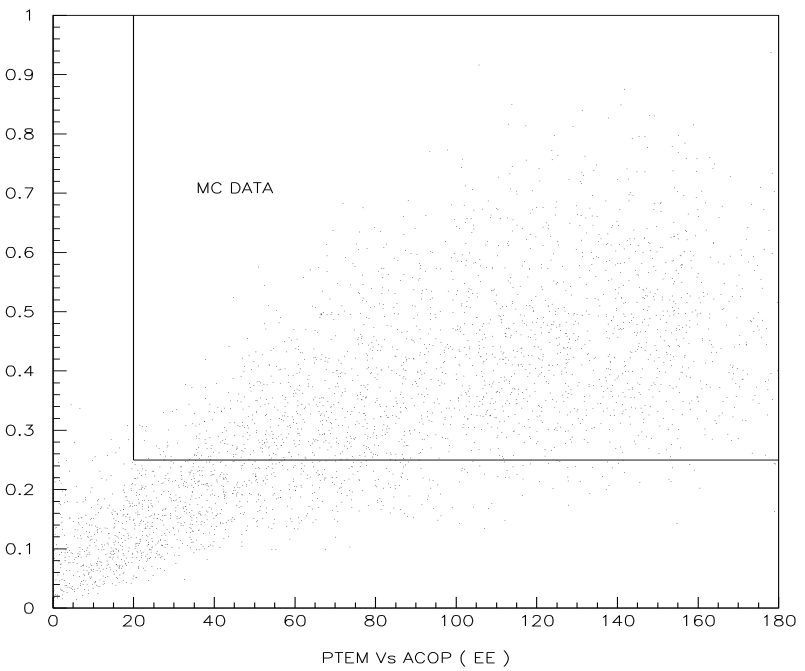

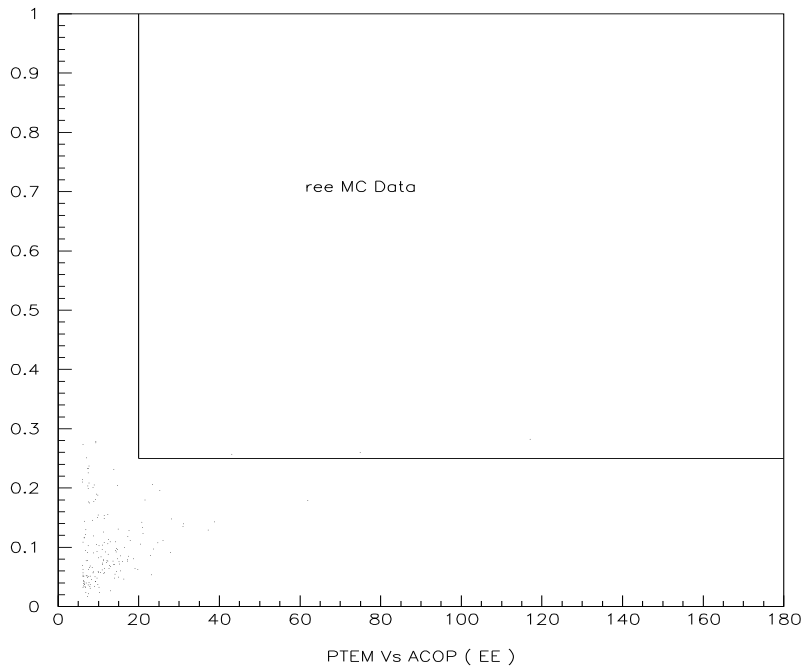

Figure 15: ee channel. Top is M. C. simulation, 10k $\tau\tau \to ee$ events; bottow is γee MC data. There are two cut lines on each plot, for $ptem \geq 0.25$ and $acop \geq 20°$. Few γee events meet the criterion for ee channel. After all cuts and normalization, there is only one ee event from 40k γee MC data, which survived.

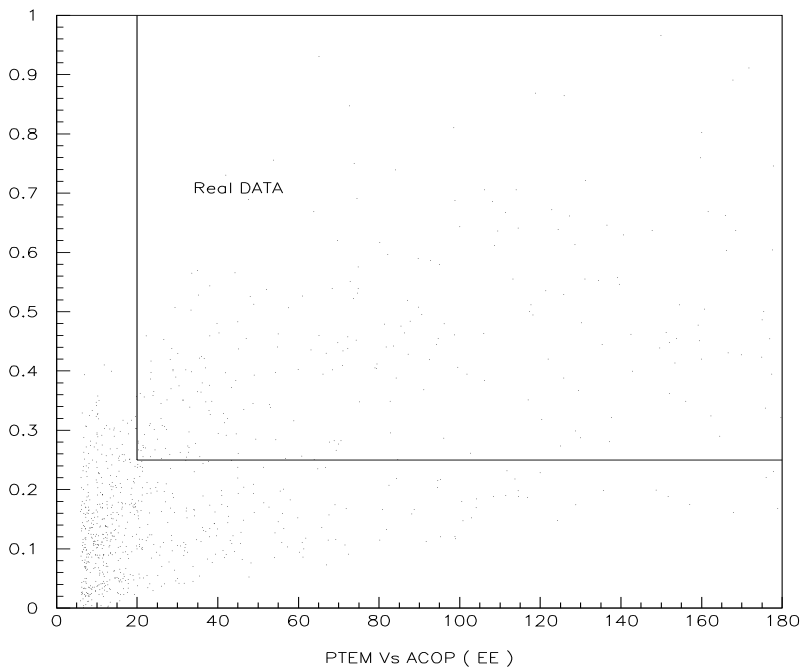

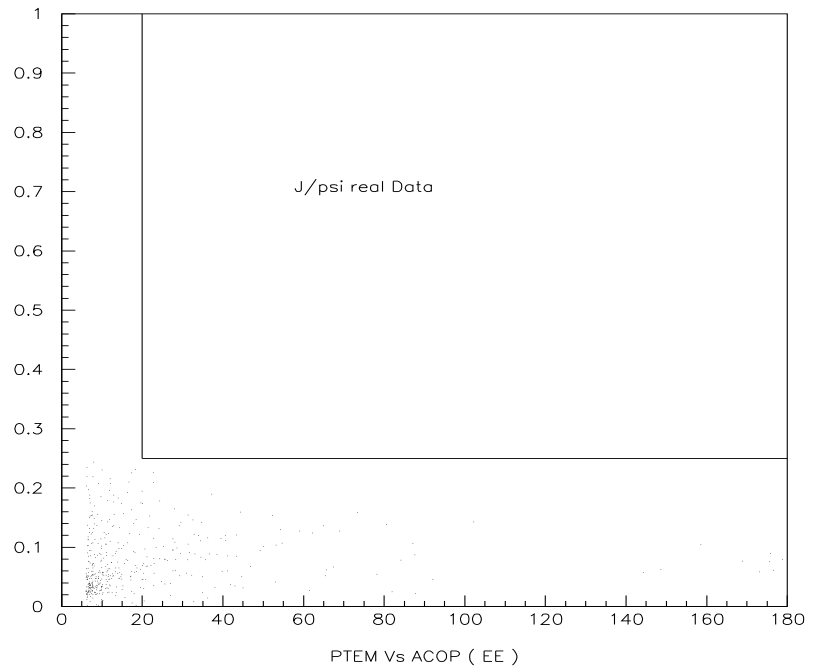

Figure 16: ee channel. Top is real 93/94 $\psi^{'}$ data; bottow is real J/ψ data, which is used to estimate $q\bar{q}$ background. There are two cut lines on each plot, for $ptem \geq 0.25$ and $acop \geq 20°$. Few events from from J/ψ meet the criterion for ee channel. After all cuts and normalization, no any events from J/ψ data meet the criterion for ee channel.

- $acop \geq 25°$;
- $10° \leq acol \leq 170°$;
- $ptem \geq 0.25$.

ee channel

- two tracks are es, those momenta required $P_{min} \leq P_e \leq P_{max}$;
- no isolated photon;
- $acop \geq 20°$;
- $10° \leq acol \leq 170°$;
- $ptem \geq 0.25$.

μh channel

- one track is a μ, the other a h, those momenta required $P_{min} \leq P_\mu \leq P_{max}, P_h lo \leq P_h \leq P_h$hi; $P_h lo = min(P_K lo, P_\pi lo), P_h hi = max(P_K hi, P_\pi hi)$;
- no isolated photon;
- $acop \geq 20°$;
- $10° \leq acol \leq 170°$;
- $ptem \geq 0.35$.

$e\rho$ channel

- one track is an e, the other a π, the momentum of e required $P_{min} \leq P_e \leq P_{max}$;
- the γs of fitting to π^0 demanded $Esc \geq 30MeV$, the angle between it and the charged track nearest to it $\theta_{open} \geq 3°$;
- the mass of π^0, and the mass and momentum of ρ required:

$$90MeV/C^2 \leq M_{\pi^0} \leq 220MeV/C^2$$
$$500MeV/C^2 \leq M_\rho \leq 1100MeV/C^2$$
$$400MeV/C \leq P_\rho \leq 1100MeV/C$$

- the system of the e and fitted ρ demanded:

$$5° \leq acol \leq 175°$$
$$10° \leq acop \leq 178°$$
$$acol + acop \geq 50°$$

- no other isolated photon, except for two photons making up π^0.

$\mu\rho$ channel

- one track is a μ, the other a π, the momentum of μ required $P_{min} \leq P \leq P_{max}$;
- the γs of fitting to π^0 demanded $Esc \geq 30MeV$, the angle between it and the charged track nearest to it $\theta_{open} \geq 3°$;
- the mass of π^0, and the mass and momentum of ρ required:

$$90MeV/C^2 \leq M_{\pi^0} \leq 220MeV/C^2$$
$$500MeV/C^2 \leq M_{\rho} \leq 1100MeV/C^2$$
$$400MeV/C \leq P_{\rho} \leq 1100MeV/C$$

- the system of the μ and fitted ρ demanded:

$$5° \leq acol \leq 175°$$
$$10° \leq acop \leq 178°$$
$$acol + acop \geq 50°$$

- no other isolated photon, except for two photons making up π^0.

3.3 The background from $q\bar{q}$

The continuum background is estimated by use of the J/ψ data, which include three datasets, those runs from 1480 to 1616, from 1750 to 1940 and from 3579 to 3738, corresponding to 5 million $q\bar{q}$ events. Only 4, 6, 0, 0, 3, and 1 events meet the criteria for $e\mu, eh, ee, \mu h, e\rho$ and $\mu\rho$ respectively, corresponding to a $R_{bgd} < 10^{-2}$.

In addition, Monte Carlo study on the two-photon process has also been performed, no background event is found.

4 Result and discussion

The items measured and the value of $N_{\tau\tau}$ obtained are listed in table 2.

Table 2 the values of items used and $N_{\tau\tau}$

mode	n	$n^{'}$	λ	$\sigma^{'}_{QED}$	$L^{'}$	ε_t	$N_{\tau\tau}$
$e\mu$	92	152	1.041	3.27	4680.9	0.99	8989.4 $\pm$ 1187.4
eh	64	109	0.892	3.27	4680.9	0.99	10302.9 $\pm$ 1622.5
ee	55	89	0.954	3.27	4680.9	0.99	10011.9 $\pm$ 1717.2
μh	42	81	0.885	3.27	4680.9	0.99	9059.1 $\pm$ 1722.5
$e\rho$	43	66	1.125	3.27	4680.9	0.99	8953.8 $\pm$ 1754.7
$\mu\rho$	36	52	1.066	3.27	4680.9	0.99	10040.7 $\pm$ 2177.0

in this table, $L^{'}(nb^{-1})$ is determined by analyzing the wide-angle Bhabha events and $\sigma^{'}_{QED}(nb)$ calculated theoretically.

The result of the weighted average for $N_{\tau\tau}$ is

$$N_{\tau\tau} = 9462.4 \pm 659.3 \pm 482.3 \tag{6}$$

where the systematic error include the contributions from the errors of $L^{'}$ ($\pm 5\%$) and ε_t ($\pm 1\%$).

Table 3 lists the differences between the previous measurement and the present check that result in the change of the value $N_{\tau\tau}$.

Table 3 changes of data and selection and their effects on $N_{\tau\tau}$

condition	present used	previous used	$\delta N_{\tau\tau}$
ψ' data	unfiltered	filtered	$\nearrow 3\%$
Ds data	93	92	$\searrow 7\%$
Esc, θ_{open} of γ	$\geq 60MeV, \geq 12^{\circ}$	$\geq 40Mev, \geq 14^{\circ}$	negligible

Furthermore, since the integrated luminosity of the Ds data has been corrected to increase by 3%, the value of $N_{\tau\tau}$ has a 3% increasement correspondingly.

In summary, all above-mentioned factors make the $N_{\tau\tau}$ reduce by about 0.9%.

If putting the values of $\sigma_{Q+I} = 2.237nb$ obtained by the theory analysis, $L = (2246 \pm 5 \pm 46)nb^{-1}$ measured by using the wide-angle Bhabha events and $N_{\psi'} = (1271 \pm 4 \pm 111) \times 10^{+3}$ measured by using a method of detecting the inclusive J/ψ production from $\psi' \to \pi^+\pi^- J/\psi$ into the formula (2), we obtain

$$Br(\psi^{'} \to \tau\tau) = (3.49 \pm 0.52 \pm 0.63) \times 10^{-3} \tag{7}$$

which is consistent with the previous value of the $Br_{\tau\tau} = (3.54 \pm 0.61 \pm 0.63) \times 10^{-3}$.

The error sources of the $Br_{\tau\tau}$ are listed in table 4.

Table 4 the error sources of the $Br_{\tau\tau}$ (%)

error source	statistical error	systematic error
$\sigma_{N_{\tau\tau}}/(N_{\tau\tau} - L \bullet \sigma_{Q+I})$	15.03	10.91
$\sigma_{\sigma_L}/(N_{\tau\tau} - L \bullet \sigma_{Q+I})$	0.25	2.33
$\sigma_{N_{\psi'}}/(N_{\psi'})$	0.31	8.73
E_{cm} and its spread	-	11.0
$\sigma_{Br_{\tau\tau}}/Br_{\tau\tau}$	15.04	17.93

The value $Br(\psi^{'} \to \tau\tau)/0.3885 = (8.93 \pm 1.34 \pm 1.60) \times 10^{-3}$ together with $Br_{ee} = (8.8 \pm 1.3) \times 10^{-3}$ and $Br_{\mu\mu} = (7.7 \pm 1.7) \times 10^{-3}$ are also in agreement with the $e - \mu - \tau$ universality hypothesis within the errors.

5 Acknowledgement

In this check, we obtain some useful helps and instructions from our colleagues at IHEP, we greatly acknowledge them. We also thank our colleagues in Hawaii University who provide us with the unfiltered reconstructed ψ' data.